


### AUTHOR QUERY FORM

 ELSEVIER	<b>Journal:</b> CHROMA  <b>Article Number:</b> 357085	<b>Please e-mail your responses and any corrections to:</b>  <b>E-mail:</b> <a href="mailto:corrections.esnl@elsevier.thomsondigital.com">corrections.esnl@elsevier.thomsondigital.com</a>
---	---	--

Dear Author,

Please check your proof carefully and mark all corrections at the appropriate place in the proof (e.g., by using on-screen annotation in the PDF file) or compile them in a separate list. Note: if you opt to annotate the file with software other than Adobe Reader then please also highlight the appropriate place in the PDF file. To ensure fast publication of your paper please return your corrections within 48 hours.

For correction or revision of any artwork, please consult <http://www.elsevier.com/artworkinstructions>.

Any queries or remarks that have arisen during the processing of your manuscript are listed below and highlighted by flags in the proof. Click on the ‘Q’ link to go to the location in the proof.

Location in article	Query / Remark: <b>click on the Q link to go</b> Please insert your reply or correction at the corresponding line in the proof
Q1 Q2 Q3 Q4 Q5	<p>Please confirm that given names and surnames have been identified correctly.</p> <p>Highlights should only consist of 85 characters per bullet point, including spaces. The highlights provided are too long; please edit them to meet the requirement.</p> <p>“Your article is registered as belonging to the Special Issue/Collection entitled “HPLC 2015”. If this is NOT correct and your article is a regular item or belongs to a different Special Issue please contact <a href="mailto:j.kastelein@elsevier.com">j.kastelein@elsevier.com</a> immediately prior to returning your corrections.”.</p> <p>One or more sponsor names and the sponsor country identifier may have been edited to a standard format that enables better searching and identification of your article. Please check and correct if necessary.</p> <p>The “Journal of Chromatography” has been split and renamed as “Chromatography A” and “Chromatography B” from volume number 652, issue number 1. Hence, all articles published in this journal in volume numbers earlier than 652, issue 1 have no A or B as part of the journal name. They have been deleted in the following references [4, 12, 14, 16]. Please check, and correct if necessary.</p> <div style="border: 1px solid black; padding: 10px; margin-top: 20px; text-align: center;"> <p>Please check this box or indicate your approval if you have no corrections to make to the PDF file</p> <input style="width: 40px; height: 25px; vertical-align: middle;" type="checkbox"/> </div>

Thank you for your assistance.



ELSEVIER

Contents lists available at ScienceDirect

## Journal of Chromatography A

journal homepage: [www.elsevier.com/locate/chroma](http://www.elsevier.com/locate/chroma)

## Highlights

**Ultra-fast high-efficiency enantioseparations by means of a teicoplanin-based chiral stationary phase made on sub-2  $\mu\text{m}$  totally porous silica particles of narrow size distribution***Journal of Chromatography A xxx (2015) pp. xxx–xxx*

Omar H. Ismail, Alessia Ciogli, Claudio Villani, Michela De Martino, Marco Pierini, Alberto Cavazzini, David S. Bell, Francesco Gasparrini\*

- Ultra-high performance teicoplanin-based stationary phase was developed on 1.9  $\mu\text{m}$  totally porous Titan silica particles.
- Ultra-fast/high efficiency chiral separations were obtained by using short (2–5-cm) and ultra-short (1 cm) columns.
- The new chiral stationary phase demonstrated wide possibilities of elution conditions: reversed phase, normal phase, polar organic mode, hydrophilic interaction liquid chromatography and sub/supercritical fluid chromatography.

Q2

UNCORRECTED PROOF



Contents lists available at ScienceDirect

## Journal of Chromatography A

journal homepage: [www.elsevier.com/locate/chroma](http://www.elsevier.com/locate/chroma)

# Ultra-fast high-efficiency enantioseparations by means of a teicoplanin-based chiral stationary phase made on sub-2 $\mu\text{m}$ totally porous silica particles of narrow size distribution<sup>☆</sup>

Omar H. Ismail<sup>a</sup>, Alessia Ciogli<sup>a</sup>, Claudio Villani<sup>a</sup>, Michela De Martino<sup>a</sup>, Marco Pierini<sup>a</sup>, Alberto Cavazzini<sup>b</sup>, David S. Bell<sup>c</sup>, Francesco Gasparrini<sup>a,\*</sup>

<sup>a</sup> Dipartimento di Chimica e Tecnologie del Farmaco, Sapienza Università di Roma, P.le Aldo Moro 5, 00185 Roma, Italy

<sup>b</sup> Dipartimento di Scienze Chimiche e Farmaceutiche, Università di Ferrara, via L. Borsari 46, 44121 Ferrara, Italy

<sup>c</sup> Sigma-Aldrich/Supelco, 595 North Harrison Road, Bellefonte, PA 16823, USA

## ARTICLE INFO

## Article history:

Received 11 September 2015

Received in revised form

20 November 2015

Accepted 23 November 2015

Available online xxx

## Keywords:

1.9  $\mu\text{m}$  Titan particles

High efficiency and ultra-fast chiral separations

Short/ultra short columns

UHPC-Titan 120-T<sub>ZWT</sub>-1.9

UHPC-chiral separations

## ABSTRACT

A new ultra-high performance teicoplanin-based stationary phase was prepared starting from sub-2  $\mu\text{m}$  totally porous silica particles of narrow size distribution. Columns of different lengths were packed at high pressure and a deep and systematic evaluation of kinetic performance, in terms of van Deemter analysis, was performed under different elution conditions (HILIC, POM, RP and NP) by using both achiral and chiral probes. For the achiral probes, the efficiency of the columns at the minimum of the van Deemter curves were very high leading to some 278 000, 270 000, 262 000 and 232 000 plates/m in hydrophilic interaction liquid chromatography (HILIC), polar organic mode (POM), normal phase (NP) and reversed phase (RP) respectively. The lowest plate height,  $H_{\min} = 3.59 \mu\text{m}$  ( $h(J) = 1.89$ ), was obtained under HILIC conditions at a flow rate of 1.4 mL/min. Efficiency as high as 200 000–250 000 plates/m (at the optimum flow rate) was obtained in the separation of the enantiomers of chiral probes under HILIC/POM conditions. N-protected amino acids,  $\alpha$ -aryloxy acids, herbicides, anti-inflammatory agents were baseline separated on short (2-cm) and ultra-short (1-cm) columns, with analysis time in the order of 1 min. The enantiomers of N-BOC-p,L-methionine were successfully baseline separated in only 11 s in HILIC mode. Several examples of fast and efficient resolutions in sub/supercritical fluid chromatography were also obtained for a range of chiral carboxylic acids.

© 2015 Published by Elsevier B.V.

## 1. Introduction

In the field of enantiomeric chromatographic separations, research has been focused on the development of very broad spectrum selectors, able to separate the largest number of chiral molecules. Unfortunately there is not yet a universal chiral selector and, while the study of new and improved selectors is still in progress, the success of enantiomeric separation is related to the availability of more columns based on different chiral selectors under different elution conditions [1–18]. Over the last ten years, the technological progress has led to the development of stationary phases on ever smaller silica particles and instruments with low

dispersion and able to reach very high pressure (up to 1500 bar): however, chiral separations have been only partly affected by these improvements. Particularly when a large number of samples is to be analyzed (i.e. in all steps of drug development process or in chiral combinatorial libraries), enantioselective HPLC is still the standard choice in the industry and remains the most usable and logical approach capitalizing on chiral screening protocols to identify the most effective chiral stationary and mobile phase combinations [19–25]. Only recently, the importance of high efficient and, at the same time, fast and ultra-fast chiral separations in the development of advanced chiral columns has been fully recognized. New approaches have been presented by using chiral stationary phases (CSPs) based on silica with reduced particle size in order to obtain even faster and faster separations [26,27]. Selectors such as  $\beta$ -cyclodextrin [28], DACH-DNB [29], Whelk-O1 [30–32], macrocyclic antibiotics [33,34] and cyclofructan derivatives [33] were covalently bonded on a new generation of sub-2  $\mu\text{m}$  totally porous (TPP) and superficially porous (SPP) silica particles.

<sup>☆</sup> Selected paper from 42nd International Symposium on High Performance Liquid Phase Separations and Related Techniques, 21–25 June 2015, Geneva, Switzerland.

\* Corresponding author.

E-mail address: [francesco.gasparrini@uniroma1.it](mailto:francesco.gasparrini@uniroma1.it) (F. Gasparrini).

Recently Supelco introduced achiral reversed phase columns packed with the new 1.9  $\mu\text{m}$  fully porous spherical silica particles (commercially known as Titan C18, 1.9  $\mu\text{m}$ ). These columns exhibit an unusual high efficiency with a reduced plate height of  $h(\lambda) = 1.7$  in narrow-bore columns [35–40].

In this work, we describe a new teicoplanin chiral stationary phase based on sub-2  $\mu\text{m}$  Titan silica particles (average pore size: 120 Å) focusing on its kinetic performances.

Teicoplanin, a macrocyclic glycopeptide, is very popular as chiral selector in HPLC due to the wide applicability in the resolution of many classes of racemates ( $\alpha$ - and  $\beta$ -amino acids, peptides,  $\beta$ -blockers,  $\beta$ -agonists, nonsteroidal anti-inflammatory agents, etc.). In fact, the unique structure of macrocyclic glycopeptides featuring a semi-rigid polypeptidic basket surrounded by sugars, ensures manifold sites and types of interaction (e.g., hydrogen bonding, ionic forces, dipole stacking,  $\pi$ - $\pi$  aromatic stacking, van der Waals interactions, hydrophobic and steric effects) [6,7,41]. By HPLC and NMR investigations, the deprotonated carboxylic group of acidic analytes was found to be pivotal in the interaction with the CSP, and almost a guarantee for the success of enantioseparation when the carboxylate fragment is close to the stereogenic center of the analyte [7]. Compounds able to fit the aglycone basket may create several hydrogen bonds through  $\text{COO}^-$  with the aglycone walls, miming the interaction, at the biological level, of the *p*-Ala-*D*-Ala terminated peptide with teicoplanin [42–46].

Very recently, Armstrong and coworkers prepared, following the traditional synthetic route, a teicoplanin-based CSP by using the new sub-2  $\mu\text{m}$  fully porous Titan particles of narrow size distribution as base material. They evaluated the performance of this phase by employing a single 50 mm  $\times$  4.6 mm (length  $\times$  I.D.) column [47]. Unlike Armstrong et al., in this work a new bonding chemistry has been used to prepare a teicoplanin-based CSP starting from the same fully porous silica particles used in [47]. The new CSP has been thoroughly characterized in terms of kinetic performance and retention mechanisms by employing columns of different geometry (10, 20, 50 and 100 mm in length with 4.6 mm I.D.) and under very different chromatographic modes including hydrophilic interaction, polar organic mode, normal phase, reversed phase and sub/supercritical fluid.

The new teicoplanin-based CSP based on sub-2  $\mu\text{m}$  totally porous silica micro-particles was found to be suitable for the separations of a broad range of analyte classes including *N*-protected amino acids,  $\alpha$ -aryloxy acids, herbicides, anti-inflammatory agents, etc., which were rapidly baseline separated. The large selectivity and, at the same time, the high achievable efficiencies has allowed for fast separations in ultra-high performance chromatography (UHPC). The successful ultra-fast/high efficiency separations by using, for the first time, short (2-cm) and ultra-short (1-cm) UHPC chiral columns were also demonstrated. In addition, it was shown that the new stationary phase can be used in all types of elution conditions: RP, HILIC, POM, NP and sub/supercritical fluid chromatography maintaining column performances when switching from one mode to another.

## 2. Experimental

### 2.1. Materials and chemicals

All reagents and solvents were purchased both from Sigma-Aldrich (St. Louis, MO, USA) and used without further purification. HPLC gradient grade solvents were filtered on 0.2  $\mu\text{m}$  Omnipore filters (Merck Millipore, Darmstadt, Germany). Chiral samples were available from previous studies or from Sigma-Aldrich (St. Louis, MO, USA). Grade 5.5 carbon dioxide (employed in sub-critical fluid chromatography) was purchased

from Gruppo SAPIO (Milano, Italy). Titan silica 1.9  $\mu\text{m}$  (pore size 120 Å, particle size 1.9  $\mu\text{m}$  and specific surface area 282  $\text{m}^2 \text{g}^{-1}$  and teicoplanin selector were a gift from Sigma-Aldrich (St. Louis, MO). Chirobiotic T columns (250 mm  $\times$  4.6 mm  $L \times$  I.D. and 50 mm  $\times$  4.6 mm  $L \times$  I.D., 5  $\mu\text{m}$  particle size) and Chirobiotic T2 column (250 mm  $\times$  4.6 mm  $L \times$  I.D., 5  $\mu\text{m}$  particle size) were provided by Sigma-Aldrich (St. Louis, MO, USA). Empty stainless steel columns, 10-cm and 5-cm long, were from IsoBar Systems by IDEX (Wertheim-Mondfeld, Germany). The 2-cm and 1-cm long columns and their holders were developed and produced in house.

### 2.2. Instruments

The UPLC Acquity Waters (Milford, MA, USA) was employed on RP, POM and HILIC conditions. This instrument includes a binary solvent manager with a maximum delivery flow rate of 2 mL/min, an auto-sampler with a 5  $\mu\text{L}$  loop injection, UV-vis programmable detector including a 500 nL flow cell, 80 Hz acquisition rate, resolution 4.8 nm and no filter time constant was used. Data acquisition, data handling and instrument control were performed by Empower 3. The maximal backpressure for the UPLC system is 1000 bar at flow rates lower or equal to 1 mL/min, and value decreases linearly, in the range 1.0–2.0 mL/min, up to 600 bar at 2 mL/min. A standard UPLC Acquity Waters column heater, in still air conditions, with a maximum temperature of 65  $^\circ\text{C}$  was used. Inlet Viper capillary of 250 mm  $\times$  100  $\mu\text{m}$  I.D. and outlet Viper capillary of 350 mm  $\times$  100  $\mu\text{m}$  I.D. were used in order to minimize the extra-column contribution. In this configuration the instrument variance was measured using a zero dead-volume connector (instead of the column). The extra-column volume (obtained by injecting uracil) was 7.22  $\mu\text{L}$  (variance,  $\sigma_{v, \text{extra}}^2 = 1.02 \mu\text{L}^2$  at 1.0 mL/min, eluent: water/acetonitrile 15/85 + 15 mM ammonium acetate,  $T$ : 35  $^\circ\text{C}$ ) [48]. A more accurate evaluation of instrumental variance as function of flow rate (range from 0.2 mL/min to 2.0 mL/min) was performed (data presented in Figure S1 of Supporting Information). The UHPLC chromatographic system used for NP evaluation was an UltiMate 3000 RS system from Thermo Fisher Dionex (Sunnyvale, CA, USA), consisting of a dual gradient RS pump (800 bar under normal phase conditions; flow rates up to 8.0 mL/min), an in-line split loop Well Plate Sampler, a thermostated RS Column Ventilated Compartment (temperature range 5–110  $^\circ\text{C}$ ) and a diode array detector (UV Vanquish detector) with a low dispersion 2.5  $\mu\text{L}$  flow cell. The UV Vanquish detector was set at a filter time constant of 0.002 s, a data collection rate of 100 Hz and a response time of 0.025 s. An additional Corona Ultra-CAD detector (data collection rate of 60 Hz and  $T_{\text{nebulizer}} = 35 \text{ }^\circ\text{C}$ ) was also used. Viper capillaries and fittings were used, with the two capillary Viper tubes (2 mm  $\times$  350 mm  $\times$  0.10 mm I.D.). Data acquisition and processing was performed with Chromeleon 6.8 software from Thermo Fisher. Detection of all tested analytes was carried out at two different wavelengths (214 nm and 254 nm). The extra-column volume (obtained by injecting uracil) of this equipment was 10.2  $\mu\text{L}$  (variance,  $\sigma_{v, \text{extra}}^2 = 3.33 \mu\text{L}^2$  at flow-rate 1.0 mL/min, eluent: water/acetonitrile 15/85 + 15 mM ammonium acetate,  $T$ : 35  $^\circ\text{C}$ ).

A Waters Acquity UPC<sup>2</sup> (ultra performance convergence chromatography) in standard configuration was used to perform SFC analyses. The system was equipped with a binary solvent delivery pump compatible with mobile phase flow rates up to 4.0 mL/min and maximum system pressure of 414 bar. A 250  $\mu\text{L}$  mixing chamber is present in the delivery system. The system also comprised an autosampler with a 10  $\mu\text{L}$  loop, a column oven compatible with temperatures up to 90  $^\circ\text{C}$  in still air conditions, a UV detector equipped with an 8  $\mu\text{L}$  flow-cell, 80 Hz acquisition rate, resolution 4.8 nm and an automated backpressure regulator (ABPR). The injector/column inlet and column/detector connection tubes were

600 mm long and had an I.D. of 0.175 mm. The extra-column volume of this instrument was estimated to be 60  $\mu\text{L}$  and the extra-column peak variance was 20–90  $\mu\text{L}^2$ , calculated from peak moments [49,50]. Data acquisition and control of the UHPSFC system were performed with the Empower 3. The ABPR was set up at 124 bar (1800 psi) for all the injections.

### 2.3. Preparation of chiral stationary phase UHPC-Titan120-T<sub>ZWIT</sub>-1.9

A proprietary bonding protocol was used to immobilize teicoplanin onto Titan-120 1.9  $\mu\text{m}$  silica particles. The bonding

chemistry provides a final CSP with alkylated and charged ammonium group on the teicoplanin skeleton at amino acid residue 1 (see Fig. 1A), thus imparting zwitterionic character to the CSP, here referred to as UHPC-Titan120-T<sub>ZWIT</sub>-1.9. The characterization of the chiral stationary phase by FT-IR provided typical bands referring to the macrocyclic antibiotic at 1658  $\text{cm}^{-1}$  and 1552  $\text{cm}^{-1}$ . The CHN analysis of phase furnished a coverage values of 12.13%C, 1.60%H and 1.35%N, corresponding to 138  $\mu\text{mol}$  of substrate per gram of silica or 0.49  $\mu\text{mol}/\text{m}^2$  (based on N).

The same batch of UHPC-Titan120-T<sub>ZWIT</sub>-1.9 was slurry packed with a pneumatically driven Haskel pump ( $P_{\text{max}}$  1000 bar) into 100  $\times$  4.6 (Column-1), 50  $\times$  4.6 (Column-2), 20  $\times$  4.6 (Column-3) and 10  $\times$  4.6 (Column-4) mm  $\times$  I.D. columns.

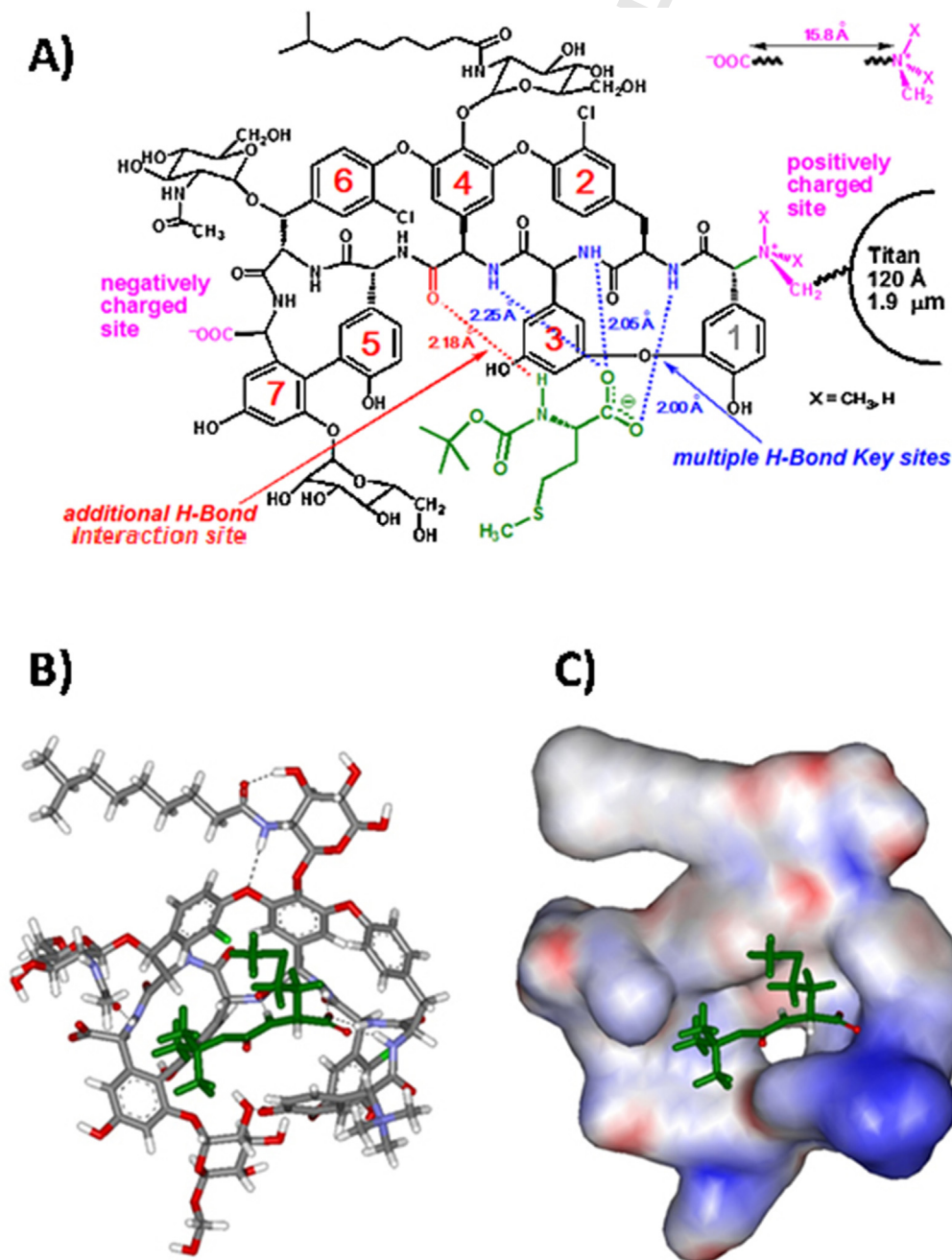


**Fig. 1.** (A) 2D structure of UHPC-Titan120-T<sub>ZWIT</sub>-1.9. Dotted lines indicate H-bonding interaction sites. (B) Polytube model of the complex between teicoplanin and N-BOC-p-Met as obtained by molecular modeling. (C) View of complex by using a surface model of teicoplanin. For interpretation of the references to color in the text, the reader is referred to the web version of this article.

## 2.4. Methodology

The performances of the new CSP were evaluated, by using all columns, in different conditions: reversed phase (RP-UHPLC), polar organic mode (POM-UHPLC), hydrophilic interaction (HILIC-UHPLC), normal phase (NP-UHPLC) and ultra-high performance sub-critical fluid chromatography (UHPSFC). All injections were performed setting a  $V_{inj}$  of 0.1–1.0  $\mu\text{L}$  in isocratic elution mode using a single solvent line, except the normal phase, where a gradient elution mode was used. Kinetic and thermodynamic evaluations were performed on each chromatographic system. The kinetic evaluation was done through the analysis of van Deemter curve starting from a minimum flow-rate of 0.1–0.5 mL/min (depending on the apparatus) up to the maximum flow-rate permitted by the instrument. All data were processed with Origin 6.0/8.0 in order to properly graph and fit the van Deemter curves. Efficiencies (N/m or plates/m), and consequently height theoretical plates ( $H$ ), were not corrected for extra-column band broadening. Measurements were repeated twice and average values were used for calculations. Hold-up time was simply estimated from the first negative deviation of the baseline trace or using an unretained marker. Detailed elution conditions and the geometry of the used columns, for sample analysis and kinetic evaluation, are reported in Table 1 and in correspondence of each presented result.

The resolution ( $R_s$ ) and efficiencies, output values from Empower 3 or Chromeleon 6.8 software, were calculated according to the European Pharmacopeia using peak width at half height ( $W_{0.5}$ ).

## 2.5. Molecular modeling calculations

Calculations were performed with the software package SPARTAN 10, v. 1.1.0 (Wave function, Inc., Irvine, CA, USA). The ground state geometry of the complex between teicoplanin and N-BOC-D-Met has been modeled by suitable modification of the relevant adduct between teicoplanin aglycone (TAG) and N-acetyl-D-phenylglycine reported in reference [7]. First, the missing portions of aglycone were added to the structure of TAG and the so obtained teicoplanin geometry was optimized by minimizing its energy with semiempirical AM1 calculations, according to the relevant algorithm implemented in SPARTAN. Then, starting from this modeled geometry of [teicoplanin-N-acetyl-D-phenylglycine] complex, the docked structure of N-acetyl-D-phenylglycine was exchanged with that of N-BOC-D-Met, ensuring that all the interactions responsible for the proposed modality of recognition were completely retained.

**Table 1**  
Overview of kinetic data obtained from van Deemter analysis. The 10-cm UHPC-Titan120-T<sub>ZWIT</sub>-1.9 column was used for the poorly retained achiral samples while a 2-cm long column for the retained chiral ones.

Elution mode	Sample	$k' (l)$	$\alpha (l)$	N/m	$H_{min} (\mu\text{m})$	$h (l)$	$\Phi (\text{mL/min})$	Mobile phase
RP	1,3-DNB	0.14	/	261 780	3.82	2.01	0.8	MeOH/H <sub>2</sub> O, 85:15 + 20 mM ammonium acetate
	14 – 1st enantiomer	5.51	/	230 950	4.33	2.28	0.4	
	14 – 2nd enantiomer	7.45	1.35	220 750	4.53	2.38	0.3	
HILIC	1,3-DNB	Unretained	/	278 170	3.59	1.89	1.4	ACN/H <sub>2</sub> O, 85:15 + 15 mM ammonium acetate
	14 – 1st enantiomer	2.36	/	250 815	3.99	2.10	0.6	
	14 – 2nd enantiomer	3.15	1.30	240 600	4.16	2.19	0.5	
	5 – 1st enantiomer	1.17	1.27	221 300	4.52	2.38	0.5	
	5 – 2nd enantiomer	1.49	/	154 900	6.46	3.40	0.5	
POM	1,3-DNB	0.04	/	270 550	3.70	1.95	2.0	ACN/MeOH, 60:40 + 0.055% CH <sub>3</sub> COOH + 0.03% TEA
	14 – 1st enantiomer	17.3	/	210 084	4.76	2.51	1.2	
	14 – 2nd enantiomer	23.1	1.34	185 300	5.40	2.84	1.2	
NP	Naphthalene	0.08	/	232 560	4.30	2.26	2.0	Hexane/EtOH, 70:30
UHPSFC	14 – 1st enantiomer	35.9	/	196 000	5.10	2.68	1.2	CO <sub>2</sub> /(MeOH/H <sub>2</sub> O 98:2 + 20 mM ammonium acetate), 60/40
	14 – 2nd enantiomer	41.2	1.16	173 300	5.77	3.04	1.0	

Finally, the resulting geometry of [teicoplanin-N-BOC-D-Met] complex was optimized by energy minimization, again resorting to semiempirical AM1 calculations.

## 3. Results and discussion

## 3.1. van Deemter analysis

van Deemter plots were recorded in different elution conditions by using either achiral, poorly retained probes in order to merely evaluate the quality of packing procedure, or using chiral probes bearing a carboxylic function which represents the key fragment involved in the association process with the selector. The experimental data are reported and summarized in Table 1 and Fig. 2 for both achiral and chiral probes. In detail, the RP-UHPLC and POM-UHPLC were firstly investigated being the typical elution conditions for teicoplanin based stationary phases. In addition, HILIC-UHPLC, NP-UHPLC and Sub-Critical Fluid conditions have been included to widen the portfolio of elution modalities and, especially for UHPSFC, to explore the potential of this new CSP in the revived SFC technique at the analytical research level. Fig. 2A refers to the loosely retained achiral probes ( $0.04 < k' < 0.14$ ) naphthalene in NP and 1,3 dinitrobenzene (1,3-DNB) in RP, POM and HILIC conditions. The van Deemter curves of achiral compounds were measured on the 10-cm long column in order to minimize the effect of extra-column peak broadening. The relevance of a low instrumental extra-column peak variance is clearly shown in Table 2 where the volume variance of columns,  $\sigma_v^2 (\mu\text{L}^2)$ , with the same geometries of those used in this work, was calculated assuming a theoretical  $H$  value of 3.8  $\mu\text{m}$  ( $H = 2d_p$ ) as function of retention factor [48]. Overall, the efficiency loss of a column due to the instrumental variance decreases when analyte retention and the column void volume increase. The green zone of Table 2 refers to cases where the combined effects of column length and analyte retention factor permit to achieve a loss of efficiency, due to extra-column peak broadening, smaller than 10% of the total peak variance. For loosely retained samples ( $k' \approx 0.05$ , achiral probes), the contribution of instrumental extra-column peak variance  $\sigma_v^2$  is negligible only with longer columns. As an example, on a 10-cm column ( $\sigma_v^2 = 1.02 \mu\text{L}^2$  at flow rate = 1.0 mL/min), the loss in efficiency due to the equipment is only about 2.5%. Irrespective of the elution conditions, the minima of the van Deemter curves showed high efficiency values, namely about 278 000, 270 000, 262 000 and 232 000 plates/m in HILIC, POM, RP and NP respectively. The lowest plate height,  $H_{min} = 3.59 \mu\text{m}$  corresponding to a reduced plate height  $h(l) = 1.89$ , was obtained under HILIC conditions at a flow rate of 1.4 mL/min.

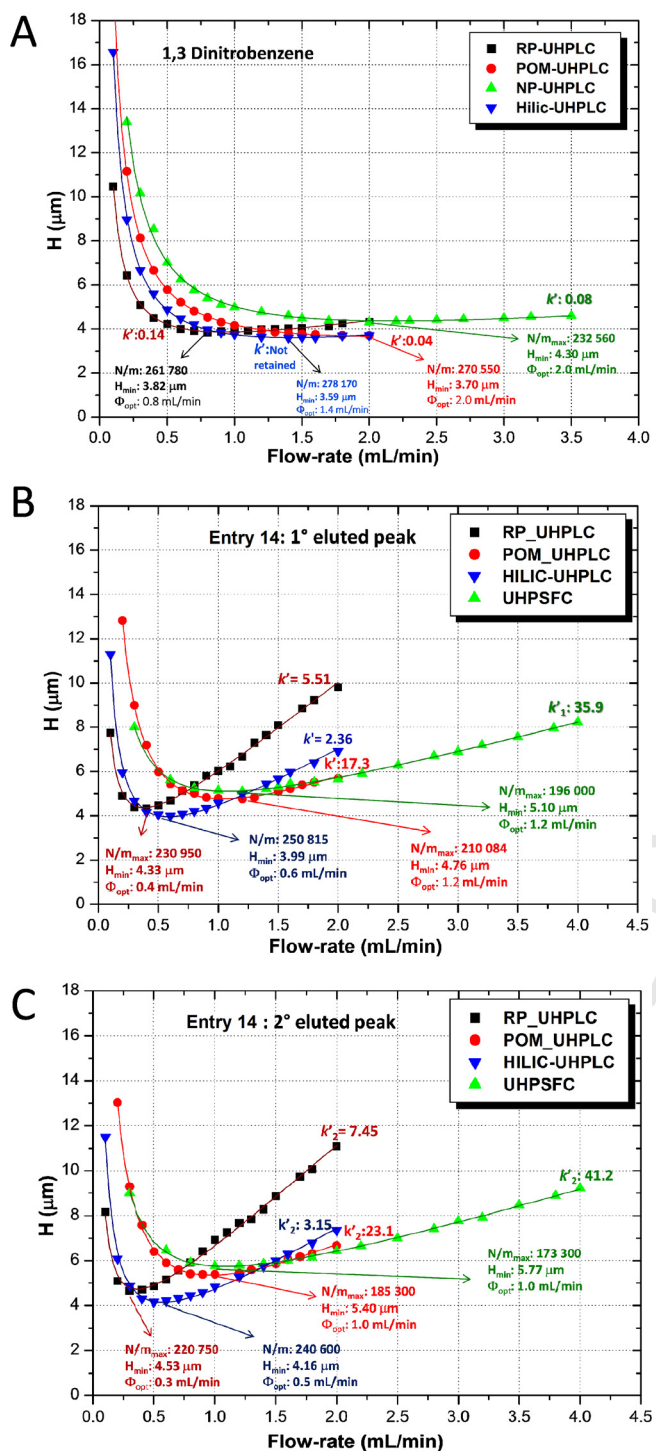


**Fig. 2.** Comparison of van Deemter plots on UHPC-Titan120-T<sub>ZWT</sub>-1.9. (A) van Deemter plots of achiral probes on 10-cm long column: 1,3-dinitrobenzene in RP (black line, MeOH/H<sub>2</sub>O 85:15, v/v + 20 mM ammonium acetate), in HILIC conditions (blue line, ACN/H<sub>2</sub>O 85:15, v/v + 15 mM ammonium acetate) and in POM mode (red line, ACN/MeOH 60:40, v/v + 0.055% CH<sub>3</sub>COOH/0.03% TEA), naphthalene in NP (green line, hexane/EtOH, v/v 70:30). van Deemter plots of chiral probes on 2-cm long column: (B) first eluted enantiomer of compound **14**; (C) second eluted enantiomer of compound **14**. RP HILIC and POM conditions are the same as for the achiral probe. UHPSFC condition (green line) was CO<sub>2</sub>/(MeOH/H<sub>2</sub>O 98:2, v/v + 20 mM ammonium acetate), 60:40. (For interpretation of the references to color in this figure legend, the reader is referred to the web version of this article.)

A similar efficiency was observed in POM elution mode with  $H_{min} = 3.70 \mu m$  and optimal flow rate of 2.0 mL/min. Notably, the minimum of the curve in RP conditions is shifted toward the "low flow-rate" zone of the plot due to the higher viscosity of

the eluent (methanol/water, 85/15, v/v) compared to the other eluting systems based on acetonitrile and hexane. In the latter cases, the lowest  $H$  values are observed at a flow rate of 0.8 mL/min. The sub-critical condition for shortly retained achiral probe was not included in this section because the high instrumental extra-column peak variance ( $\lambda_{20-90} \mu L^2$ , calculated from peak moments [49,50]) prevented meaningful measurements. A comparison between the kinetic behavior of the column packed with the new 1.9  $\mu m$  CSP and that of a commercially available Chirobiotic T2 column packed with 5.0  $\mu m$  CSP was carried out under RP conditions using 1,3-DNB as a probe (Fig. S2, supporting information). Notable differences were the lower plate counts for the column packed with the 5.0  $\mu m$  CSP, reaching  $N/m = 54\ 570$  at the optimal flow rates of 0.6 mL/min compared to  $N/m = 261\ 780$  for the column packed with the 1.9  $\mu m$  CSP at the optimal flow rate of 0.8 mL/min. The  $H_{min}$  value for the 5.0  $\mu m$  column is 18.33  $\mu m$  corresponding to  $h(\lambda) = 3.66 \mu m$  vs.  $H_{min} = 3.82 \mu m$  corresponding to  $h(\lambda) = 2.01$  for the 1.9  $\mu m$  column. In addition, the C-branch of the van Deemter curve for the 1.9  $\mu m$  column is almost flat up to the maximum flow rate explored of 1.6 mL/min, whereas a steeper rise of the van Deemter curve was observed for the 5.0  $\mu m$  column under the same experimental conditions.

van Deemter plots for chiral probes are shown in Fig. 2B and C for the first and second eluted enantiomers of compound **14**, respectively, for both enantiomers in RP-UHPLC, UHPSFC, POM-UHPLC and HILIC-UHPLC conditions by using a 2-cm column. In this case, accurate van Deemter analysis was possible in spite of the small column length, because the large retention factors of the chiral probes minimized the effect of the instrument variance (see Table 2). Indeed, when the same analysis was performed on an equipment optimized to reduce the extra-column volume (by using 75  $\mu m$  I.D.  $\times$  350 mm inlet and outlet Nano Viper connecting tubes), essentially the same efficiency was achieved, at the cost of increased system back-pressure (data not shown).

For the first eluted enantiomer of **14** we found efficiency values at the optimal flow rate in the range 196 000–250 815 plates/m. The lowest plate height,  $H_{min} = 3.99 \mu m$  was observed under HILIC conditions at a flow rate of 0.6 mL/min. When looking at the eluent flow rates yielding the best kinetic performances for the different elution conditions, we observe that HILIC is favored in the range between 0.4 and 1.2 mL/min, followed by POM from 1.3 to 2.0 mL/min and eventually by UHPSFC up to 4.0 mL/min.

On the other hand, for the second eluted enantiomer of **14** we found efficiency values at the optimal flow rate in the range 173 300–240 600 plates/m. The lowest plate height,  $H_{min} = 4.16 \mu m$  was observed under HILIC conditions at a flow rate of 0.5 mL/min. The second eluted enantiomer of **14** showed two preferred elution conditions: HILIC with eluent flow rates spanning from 0.4 to 1.4 mL/min and UHPSFC above 1.4 mL/min.

Comparison of the van Deemter curves in Fig. 2B and C shows that the efficiencies recorded for the two enantiomers of **14** are very similar under HILIC and RP conditions, whereas those recorded for the first eluted enantiomer are consistently larger under POM-UHPLC and UHPSFC conditions. The optimal flow rates for the second eluted enantiomer are always found at slightly lower values compared to the first eluted one.

For both enantiomers, and for the achiral probe, we note the lowest efficiency values are recorded under UHPSFC conditions, a finding that is partly related to the high extra column instrumental variance. In addition, the high MeOH content in the sub-critical eluent increases its viscosity and contributes to worsen the kinetic performances of the column. For both enantiomers of **14**, but not for the achiral probe, we observe that under RP the efficiency rapidly degrades by increasing the flow rate. In fact, when the

**Table 2**

Column volume variances,  $\sigma_v^2$ , as function of retention factor taking into account a theoretical  $H$  of  $2d_p$ . Internal diameter: 4.6 mm;  $H_{\text{theo}} = 2d_p$ ;  $N$ :  $L/H_{\text{theo}}$ ;  $r$ : internal radius;  $\sigma_v^2$  ( $\mu\text{L}^2$ ): variance of column  $\sigma_{v,\text{extra}}^2$  ( $\sigma_v^2 = \frac{w_{30}^2}{5.545}$ ) [48].

$L$ (mm)	$d_p$ ( $\mu\text{m}$ )	$H_{\text{theo}}$ ( $\mu\text{m}$ )	$N$ ( $l$ )	I.D. (mm)	$r$ (mm)	$\varepsilon_l$ ( $l$ )	$\sigma_v^2$ ( $k=0.05$ )	$\sigma_v^2$ ( $k=0.5$ )	$\sigma_v^2$ ( $k=1$ )	$\sigma_v^2$ ( $k=2$ )	$\sigma_v^2$ ( $k=3$ )	$\sigma_v^2$ ( $k=5$ )
10	1.9	3.8	2632	4.6	2.3	0.6	4.17	8.50	15.11	34.00	60.45	136.02
20	1.9	3.8	5263	4.6	2.3	0.6	8.33	17.00	30.23	68.01	120.91	272.04
50	1.9	3.8	13158	4.6	2.3	0.6	20.83	42.51	75.57	170.02	302.26	680.10
100	1.9	3.8	26316	4.6	2.3	0.6	41.66	85.01	151.13	340.05	604.53	1360.19

flow rate is doubled respect to the optimum value of 0.4 mL/min, the efficiency decreases by about 30%. However, the large resolution obtained in this elution conditions (see below) still allow fast runs to be performed. In addition to the enantiomers of compound **14**, the enantiomers of N-BOC-D,L-Met **5** were also investigated by van Deemter analysis (Fig. S3). Interestingly, the curve of the first eluted enantiomer of **5** and those of both enantiomers of **14** are nearly overlapped, while the curve of the second eluted enantiomer of **5** is considerably and constantly shifted to higher  $H$  values (lower efficiency): at the optimal flow rate of 0.5 mL/min, the  $H_{\text{min}}$  values are 4.52  $\mu\text{m}$  and 6.46  $\mu\text{m}$  for the first and second eluted enantiomer, respectively. A plausible explanation of this sizeable loss in efficiency can be envisioned considering a slower, stereochemical dependent selector-selectand association process.

As already suggested by molecular modeling investigation [7], and further confirmed by the inspection of the X-ray structures of complexes involving teicoplanin and carboxy-terminal p-Ala-D-Ala peptide derivatives [42,44,45], the general association mechanism operated by teicoplanin toward ligands bearing a carboxylate fragment entails the formation of several hydrogen bonds between the analyte and the peptide backbone of the immobilized antibiotic. Among them, at least three interactions are involved between the following pairs of atoms: the backbone amide NH of residue 2 and one carboxylic acid O atom of the analyte, the backbone amide NHs atoms of residues 3 and 4 and the other O atom of the carboxylate group of the analyte (Fig. 1) [42,44,45].

An additional fourth H-bound, whose strength is much more dependent on the stereochemistry of the analyte, is also established by the carbonyl O atom (red in structure of Fig. 1A) of teicoplanin residue 4, close to the carboxylate binding pocket, and the amide NH atom of the peptide-type analyte, so giving a further important contribution to the stabilization of the analyte/teicoplanin complex [6,42,44]. This new, strong interaction, can more specifically act by modulating the global host/guest recognition, bringing the portion of the analyte bound to the amide NH moiety in close contact with the left pocket of teicoplanin, in a way that strongly depends on the stereochemistry of the guest. Thus, it is obviously expected that, a more effective and strong host/guest network of interactions should lead to a slower analyte/teicoplanin adsorption-desorption process and, consequently, from the chromatographic viewpoint, to an appreciable loss in efficiency, as in fact it is pointed out by the peak broadening of the most retained D enantiomer of N-BOC-p,L-Met. On the contrary, the steric constraints that prevent an equivalent large retention for the L enantiomer of N-BOC-p,L-Met may be assumed responsible for a faster adsorption-desorption kinetics, which leads to the sharper peak observed for N-BOC-L-Met.

### 3.2. Applications on UHPC-Titan120-T<sub>ZWIT</sub>-1.9 and scale-down in column length for rapid separations

The overall behavior of the new CSP, its potential use in fast analysis with short columns and its wide elution mode versatility are clearly illustrated by Table 3, where retention, selectivity, resolution values and elution times are gathered for a collection of structurally diverse chiral analytes. Representative enantiomeric separations include those of N-protected amino acids and of other acidic ( $\alpha$ -aryloxy acids, haloxyfop, ketorolac and mandelic acid) and polar (sulfoxide and phosphine oxide) samples. Enantioseparations of all amino acid derivatives (entries 1–13, namely N-Fmoc-, N-BOC-, N-Z- and N-Dansyl-protected amino acids) were realized in RP, on 10-cm long column and provided resolution values spanning from 2.25 to 10.7, except for the entry 13 ( $R_s = 1.15$ ). Efficiencies of the first eluted enantiomers ranged from 80001 N/m (entry 3) to 111620 N/m (entry 5). Notably, the high efficiency values were maintained also in the case of the second eluted enantiomer. A remarkable efficiency decrease was recorded only for the second eluted D enantiomer of N-Fmoc-p,L-Ala **1**, N-Fmoc-D,L-Leu **4** and N-Z-D,L-Leu **8**. In fact, the peak efficiency of the more retained enantiomers of **4** and **8** was one-half of those obtained for the less retained ones, while the peak efficiency of the more retained enantiomer of **1** was one-third of that of the less retained. Taking into account the potential of this CSP based on 1.9  $\mu\text{m}$  totally porous silica particles for fast analysis, all separations obtained on the 10 cm column showing  $R_s > 6.0$  were moved to shorter 2-cm and 1-cm long columns. The transition from 10 to 2 and 1-cm long columns allows a consistent reduction of analysis times (under 60 s for 1-cm long column) preserving resolution values  $R_s > 1.63$ , thus offering a rapid separations tool that is highly desired e.g. for high-throughput screening of chiral drugs. Downsizing of columns should not alter their kinetic performance in terms of plates/m count. For reasons given before, a reduction in either internal diameter or length can cause an efficiency loss. While the impact of lower internal diameters on efficiency is substantial (wall effect) [51], moving to lower column lengths at constant internal diameter leaves efficiency unaffected, and a good packing procedure guarantees the proportionality between column length and plate per column count. In fact, by analyzing the chromatographic profiles of ketorolac and haloxyfop (Fig. 3) obtained on columns of 1-cm, 2-cm and 5-cm lengths, high values of efficiencies were recorded in the range of about 1300–7850 plate per column for the second eluted enantiomers (Fig. 3A and Table S1 of Supporting Information). A correct correlation between plates/column values and column length was also observed achieving very similar plates/m efficiencies independently from the column length (see plates/m values for each column format, Fig. 3B). Moreover, the three columns are



**Table 3**  
Chromatographic data for chiral separations on UHPC-Titan120-T<sub>ZWIT</sub>-1.9.

Entry/name	Structure	N <sub>1</sub> /m	N <sub>2</sub> /m	k' <sub>1</sub>	k' <sub>2</sub>	t <sub>r,2</sub> (min)	α	Rs	Flow-rate (mL/min)
<b>1</b> Fmoc-D,L-Ala		104 730 <sup>1,a</sup>	35 140	5.46	11.2	9.36	2.20	10.7	1.0
		76 400 <sup>3,a</sup>	36 000	"	"	1.55	"	4.03	2.0
		79 890 <sup>4,a</sup>	36 090	2.80	3.74	0.85	"	3.02	2.0
		91 700 <sup>3,b</sup>	43 650	2.80	3.74	0.57	1.34	1.91	2.0
<b>2</b> Fmoc-D,L-Ser		93 528	71 470	3.25	4.28	4.05	1.32	4.85	1.0
<b>3</b> Fmoc-D,L-Gln		80 001 <sup>1,a</sup>	56 810	3.66	6.40	5.66	1.75	9.12	1.0
		62 950 <sup>3,a</sup>	50 850	"	"	1.32	"	2.69	2.0
		67 510 <sup>4,a</sup>	53 740	3.19	4.04	0.74	"	2.20	2.0
		135 000 <sup>3,b</sup>	121 100	3.19	4.04	0.94	1.27	2.34	1.5
		107 250 <sup>3,b</sup>	94 700	3.19	4.04	0.70	"	2.12	2.0
<b>4</b> Fmoc-D,L-Leu		95 180 <sup>1,a</sup>	46 510	2.45	4.54	4.24	1.85	9.00	1.0
		71 350 <sup>3,a</sup>	50 800	"	"	0.93	"	3.28	2.0
		73 800 <sup>4,a</sup>	52 520	1.06	1.40	0.51	"	2.47	2.0
		133 500 <sup>3,b</sup>	106 450	1.06	1.40	0.45	1.33	1.89	1.5
		106 500 <sup>3,b</sup>	81 400	1.06	1.40	0.34	"	1.71	2.0
<b>5</b> BOC-D,L-Met		111 620 <sup>1,a</sup>	98 145	1.73	2.51	2.69	1.45	6.39	1.0
		100 150 <sup>3,a</sup>	87 000	1.18	1.49	0.54	"	2.20	2.0
		107 020 <sup>4,a</sup>	93 360	1.18	1.49	0.30	"	1.63	2.0
		130 800 <sup>3,b</sup>	112 650	1.18	1.49	0.36	1.28	1.71	2.0
<b>6</b> BOC-D,L-Phe		106 270 <sup>1,a</sup>	100 230	1.98	2.28	2.51	1.15	2.45	1.0
<b>7</b> BOC-D,L-Trp		91 760 <sup>1,a</sup>	82 300	2.93	3.32	3.31	1.13	2.25	1.0
<b>8</b> Z-D,L-Leu		98 420 <sup>1,a</sup>	55 470	2.49	4.15	3.96	1.99	10.4	1.0
		86 850 <sup>3,a</sup>	60 650	"	"	0.81	"	4.02	2.0
		73 800 <sup>4,a</sup>	52 600	2.49	4.15	0.51	"	2.47	2.0
<b>9</b> Z-D,L-Phe		82 120 <sup>1,a</sup>	46 970	3.17	4.37	4.11	1.38	4.82	1.0
<b>10</b> Dansyl-D,L-Met		88 780 <sup>1,a</sup>	65 610	3.24	5.67	5.11	1.75	9.58	1.0
		69 950 <sup>3,a</sup>	56 950	"	"	1.30	"	3.13	2.0
		72 650 <sup>4,a</sup>	59 430	1.19	1.79	0.73	"	2.28	2.0
		131 900 <sup>3,b</sup>	102 800	1.19	1.79	0.52	1.79	2.89	1.5
		108 100 <sup>3,b</sup>	83 150	1.19	1.79	0.40	"	2.65	2.0
<b>11</b> Dansyl-D,L-Phe		85 700 <sup>1,a</sup>	75 920	3.81	4.46	4.18	1.17	2.77	1.0

Table 3 (Continued)

Entry/name	Structure	N <sub>1</sub> /m	N <sub>2</sub> /m	k' <sub>1</sub>	k' <sub>2</sub>	t <sub>r,2</sub> (min)	α	Rs	Flow-rate (mL/min)
12 Dansyl-D,L-Leu		99 540 <sup>1,a</sup>	91 570	2.74	3.17	3.20	1.16	2.49	1.0
13 Dansyl-D,L-Thr		99 340 <sup>1,a</sup>	95 709	2.90	3.09	3.13	1.07	1.15	1.0
14		126 700 <sup>3,a</sup>	114 600	5.51	7.45	1.41	1.35	3.16	1.5
		176 240 <sup>3,b</sup>	166 940	2.36	3.15	0.75	1.30	-	1.5
		193 450 <sup>3,c</sup>	164 900	17.3	23.1	3.88	1.34	4.08	1.5
		119 650 <sup>3,d</sup>	101 150	35.0	40.6	2.71	1.16	1.70	4.0
15		125 800 <sup>3,a</sup>	102 300	5.56	8.35	1.62	1.50	4.15	1.5
		173 550 <sup>3,b</sup>	153 150	1.69	2.66	0.68	1.58	4.36	1.5
		189 500 <sup>3,c</sup>	143 200	13.6	20.3	3.45	1.50	5.31	1.5
		114 350 <sup>3,d</sup>	89 450	21.3	27.9	1.97	1.31	2.91	4.0
16		119 850 <sup>3,a</sup>	108 850	4.72	5.62	0.87	1.19	1.76	1.5
		166 900 <sup>3,b</sup>	155 800	1.42	1.70	0.50	1.19	1.53	1.5
		177 450 <sup>3,c</sup>	165 950	10.7	12.7	2.25	1.20	2.29	1.5
		100 300 <sup>3,d</sup>	78 850	13.2	14.6	1.06	1.10	0.94	4.0
17 Haloxypop		148 800 <sup>3,a</sup>	133 800	3.77	5.84	2.25	1.55	4.55	0.7
		(81 100) <sup>3,a</sup>	(70 650)	(-)	(-)	(1.10)	(-)	(3.35)	(1.5)
		169 650 <sup>3,c</sup>	148 700	11.5	16.0	2.72	1.40	4.32	1.5
		87 200 <sup>3,d</sup>	76 600	18.0	23.3	1.67	1.29	2.46	4.0
18 Mandelic acid		106 750 <sup>3,a</sup>	25 650	6.51	22.5	3.96	3.45	6.67	1.5
		161 900 <sup>3,b</sup>	102 550	3.17	8.96	1.90	2.83	9.90	1.5
		158 100 <sup>3,c</sup>	100 350	26.2	64.2	10.4	2.45	9.83	1.5
		868 00 <sup>3,d</sup>	26 700	74.1	200	13.9	2.70	6.02	4.0
19 Ketorolac		104 900 <sup>3,a</sup>	98 750	6.13	8.95	1.78	1.46	2.78	1.5
		150 850 <sup>3,c</sup>	146 900	22.7	32.7	4.58	1.44	2.57	1.5
		782 00 <sup>3,d</sup>	72 850	22.9	31.7	2.36	1.38	2.69	3.5
		/	/	/	/	/	/	/	/
20		/	/	1.47 <sup>2,e</sup>	1.69	1.25	1.15	1.76	1.5
21		/	/	3.96 <sup>2,e</sup>	4.22	2.43	1.07	1.23	1.5
22 *meso compound		/	/	8.62 <sup>2,e</sup>	12.110.3*	6.11	1.41	4.71	1.5
23 Sulfoxide 4		/	/	5.80 <sup>e</sup>	7.54	5.10	1.30	6.02	1.5
24 Phosphine oxide		/	/	4.59 <sup>2,e</sup>	4.85	2.72	1.06	0.86	1.5

Notes: Column geometry: <sup>1</sup>100 mm × 4.6 mm; <sup>2</sup>50 mm × 4.6 mm; <sup>3</sup>20 mm × 4.6 mm, <sup>4</sup>10 mm × 4.6 mm.Eluents: <sup>a</sup>MeOH/H<sub>2</sub>O 85:15 + 20 mM CH<sub>3</sub>COONH<sub>4</sub> (RP); <sup>b</sup>ACN/H<sub>2</sub>O 85:15 + 15 mM CH<sub>3</sub>COONH<sub>4</sub> (HILIC); <sup>c</sup>ACN/MeOH 60:40 + 0.055% acetic acid + 0.03% triethylamine (POM); <sup>d</sup>CO<sub>2</sub>/(MeOH/H<sub>2</sub>O 98:2 + 20 mM CH<sub>3</sub>COONH<sub>4</sub>) 60:40 (SFC); <sup>e</sup>A: Hex/EtOH 95:5, B: hexane/EtOH/MeOH 50:45:5 (NP, gradient: 0' 100/0; 5' 40/60; 6' 40/60; 6.1' 0/100; 7.1' 0/100; 7.5' 100/0).

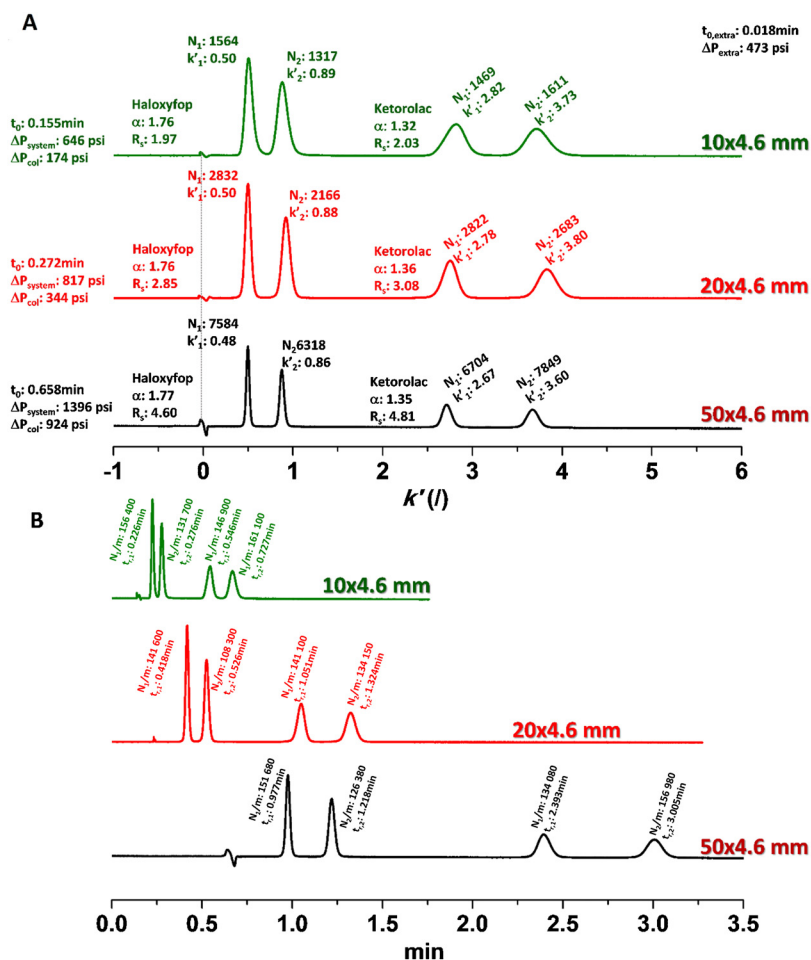


**Fig. 3.** Separations of haloxyfop and ketorolac on 1-cm, 2-cm and 5-cm UHPC-TE<sub>2</sub>WIT-1.9 in HILIC condition. (A) Chromatograms normalized on the retention factor ( $k'$ ) on x-axis in order to have a thermodynamic evaluation irrespective of column geometry. (B) Standard chromatographic traces with retention time (on x-axis). Eluent: ACN/H<sub>2</sub>O 85:15 + 15 mM ammonium acetate; flow-rate: 1.0 mL/min; T: 35 °C.

equivalent from the thermodynamic point of view (same  $k'$  and  $\alpha$ ), as it is evident from Fig. 3A, where chromatographic traces are reported as a function of retention factor. Indeed, these results confirm the high homogeneity of the packed bed of each column and a true achievable scale-down procedure. The majority of analyzed samples (entries 1–19) were well resolved by using three chromatographic modes (RP, POM and UHPSFC) attesting the versatility of new stationary phase. Some of them were analyzed also in HILIC mode at 1.5 mL/min and 2.0 mL/min achieving the shortest analysis times. Resolutions in entries 20–24 have required NP conditions performed in gradient elution mode with resolutions ranging from 0.86 to 6.02. Representative chromatograms obtained in different elution conditions are reported in Fig. 4. High efficiencies and good peak symmetry were recorded, even for very polar analyte like mandelic acid **18** and sulfoxide **23** (Fig. 4E, H) in normal phase elution. The ability to use the CSP in different elution conditions can be advantageous to modulate the retention and enantioselectivity of samples, especially if they are strongly retained. As an example, the enantioseparation of mandelic acid **18** was accomplished in 2 min by using HILIC-UHPLC with a 5-fold gain in analysis time respect to the POM-UHPLC (Fig. S4).

Resolution values in entries 14–16 refer to a set of analytes with 2-aryloxy-propionic acid structure, differing in the alkyl group on the stereogenic center. Fig. 5A shows the chromatograms recorded on the 2.0 cm × 0.46 cm L × I.D. column using 1.5 mL/min flow rate in polar organic mode that furnished the best results in terms of plates/m (193 450, 189 500 and 177 450 N/m for the first eluted

enantiomers of **14**, **15** and **16** respectively). To evaluate the effect of the flow-rate on efficiency, the enantiomers of  $\alpha$ -aryloxy acid **14** were resolved using flow-rates of 1.0, 1.5 and 2.0 mL/min in polar organic mode (Fig. 5B). As expected from the relatively flat C-branches of the van Deemter plots (Fig. 2), the efficiency was only partially affected by increasing flow-rate. In fact, at the optimal flow-rate of 1.0 mL/min, the efficiency was 208 850 N/m for the first eluted enantiomer with a resolution of 4.18 and the analysis was completed in 6.5 min, delivering the eluent twice faster we observed an efficiency value of N/m = 175 440 for the same peak with a resolution of 3.93, and a shortened analysis time of 3 min. Focusing on efficiency, run time and resolution, we found that a flow-rate of 1.5 mL/min was the best compromise between all these factors: compared to the optimal flow rate, the efficiency loss was only 7%, the resolution dropped only by 2% but a consistent reduction of run time, about 40%, was observed.

### 3.3. Moving to ultra-fast separations by using the 1-cm long column

The transfer to faster analysis can be properly done using the following well known equation:

$$t_r = \frac{L}{\mu_0} (1 + k')$$

which connects the retention time of a generic analyte to the: geometrical (column length,  $L$ ), kinetic (linear velocity,  $\mu_0$  as

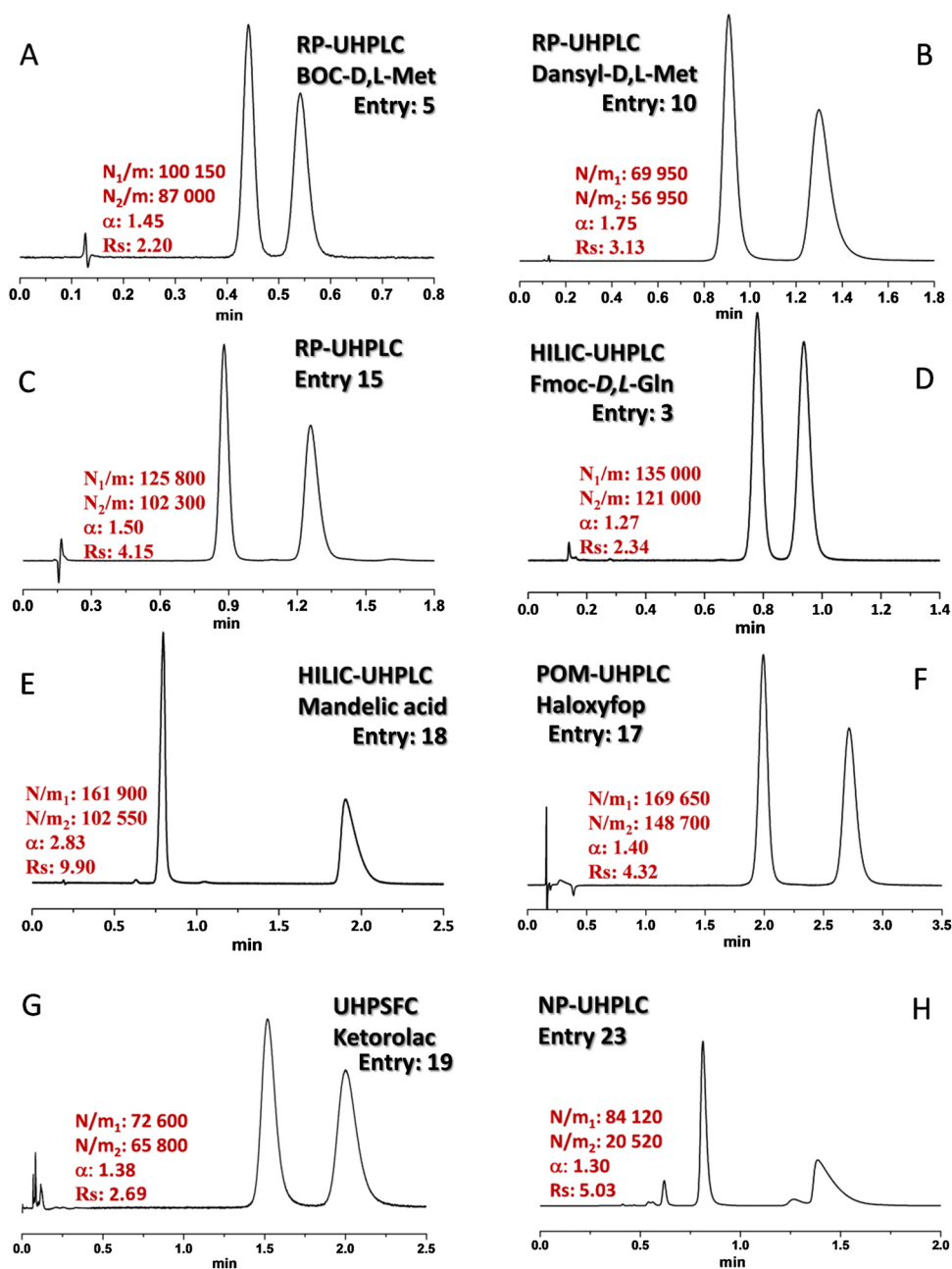


**Fig. 4.** Enantioseparations in different elution modes at  $T: 35^{\circ}\text{C}$ . Column: *UHPC-Titan120-T<sub>ZWIT</sub>-1.9*, 2.0 cm  $\times$  0.46 cm. (A) N-BOC-D,L-Met **5**, (B) N-Dansyl-D,L-Met **10** and (C) compound **15** in RP (flow-rate: 1.5 mL/min; MeOH/H<sub>2</sub>O 85:15 + 20 mM ammonium acetate). (D) N-Fmoc-Gln **3** and (E) mandelic acid **18** in HILIC (flow-rate: 1.5 mL/min; ACN/H<sub>2</sub>O 85:15, v/v + 15 mM ammonium acetate). (F) POM elution (flow-rate: 1.5 mL/min; ACN/MeOH 60:40, v/v + 0.055% CH<sub>3</sub>COOH/0.03% TEA) for haloxyfop **17**. (G) Ketorolac **19** in sub-critical fluid chromatography (flow-rate: 4.0 mL/min; CO<sub>2</sub>/A 60:40; A: MeOH/H<sub>2</sub>O 98:2 + 20 mM CH<sub>3</sub>COONH<sub>4</sub>). (H) Compound **23** in NP (flow-rate: 1.5 mL/min; hexane/(EtOH/MeOH 80:20) 50:50).

column length/dead time,  $k(t_0)$  and thermodynamic (retention factor,  $k'$ ) parameters. Combining the use of short columns (which produce only short analysis times) and CSP developed on sub-2  $\mu\text{m}$  particles (high efficient media), the ultra-high performance chiral separations are in principle possible. Moreover, a realistic ultra-high performance chiral separation should be associated with a suitable value of enantioselectivity. In this work, high resolutions were also recorded on the 2-cm long *UHPC-Titan120-T<sub>ZWIT</sub>-1.9* (see Table 3, a and b elution conditions). With the aim to further reduce the analysis time maintaining a baseline separation, a 1-cm long column was designed and packed in house into special holder in house developed. The N-protected amino acids, which gave

resolution values greater than 6 on 10-cm long column in RP-UHPLC, were well separated generally in less than 100 s on this very short column (see Table 3). The chromatographic data obtained for entries **5** and **14–19** on 1-cm column are summarized in Table 4 and Fig. 6. Fast enantioseparations were achieved in RP-UHPLC, HILIC-UHPLC and POM-UHPLC at 2.0 mL/min, the maximum allowable instrumental flow rate, and in subcritical fluid condition-UHPSFC at 4.0 mL/min. In Fig. 6A the fastest separations in RP-UHPLC are reported and all runs were completed in less than 50 s. The enantiomers of **16** and of N-BOC-D,L-Met **5** were well separated in 18 s with a  $R_s$  values of 1.21 and 1.63 respectively. A remarkable high resolution of 2.51 was recorded for haloxyfop **17** with an

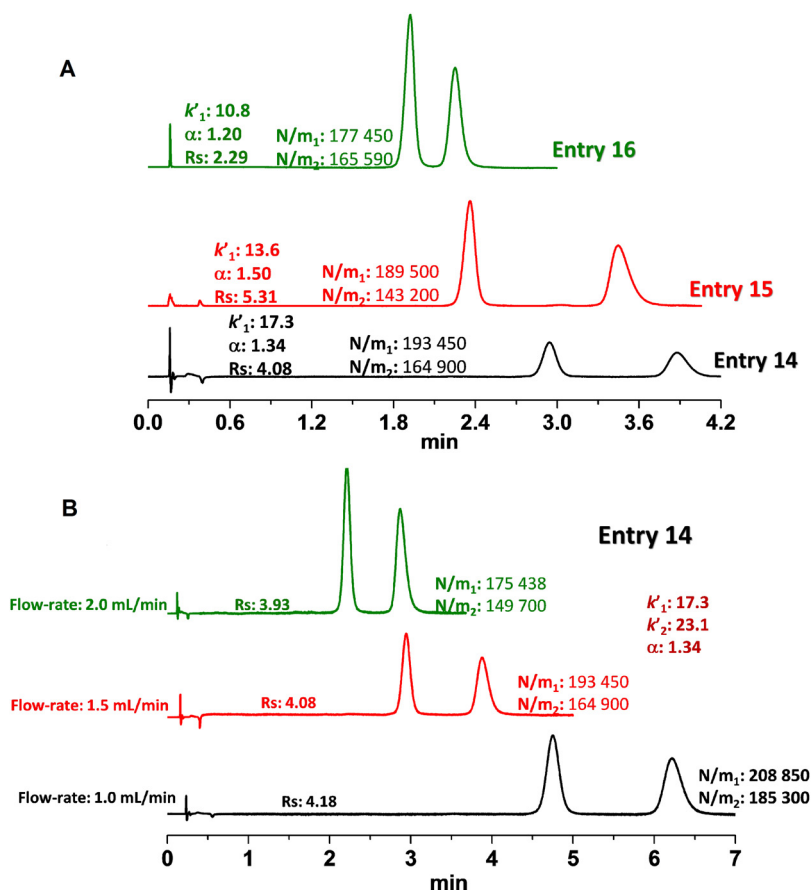


**Fig. 5.** (A)  $\alpha$ -Aryloxy acids **14**, **15** and **16** (black, red and green traces respectively) enantioresolutions in polar organic mode (ACN/MeOH 60:40 + 0.055%  $\text{CH}_3\text{COOH}$  + 0.03% TEA) on the  $2.0\text{ cm} \times 0.46\text{ cm}$  column. (B)  $\alpha$ -Aryloxy acid **14** at different eluent flow-rates: 1.0 mL/min, 1.5 mL/min and 2.0 mL/min, black, red and green traces respectively. (For interpretation of the references to color in this figure legend, the reader is referred to the web version of this article.)

elution time of 24 s. Switching in POM-UHPLC and UHPSFC modes, the analysis times are a little bit higher (70–120 s, Table 3). However, as expected by the higher optimal flow rates observed on the van Deemter curve compared to those observed for RP mode, we observed higher efficiencies, mainly in POM-UHPLC. Representative ultra-fast chromatograms are reported in Fig. 6B. The fastest

overall enantioseparation was achieved for N-BOC-p,L-Met **5** in HILIC mode in only 11 s. Haloxyfop **17** was resolved in 73 s with an extremely high resolution value of 3.19 and almost 160 000 N/m measured on the first eluted enantiomer. Short separation times can be obtained also by using sub-critical fluid conditions. In this case, the relatively favorable eluent viscosity enables high flow rates without experiencing high back-pressure issues. Separations of  $\alpha$ -aryloxy acid **15** and ketorolac **19** were completed in less than 70 s with  $R_s$  of 2.15 and 2.45, respectively at a flow rate of 4.0 mL/min.

**Table 4**  
Ultra-fast separations by using 1-cm UHPC-Titan120-T<sub>ZWIT</sub>-1.9 column.

Entry	N <sub>1</sub> /m	N <sub>2</sub> /m	t <sub>r,2</sub> (s)	R <sub>s</sub>	Flow-rate (mL/min)
<b>5</b>	129 220 <sup>b</sup>	92 420	11	1.04	2.0
	107 900 <sup>a</sup>	93 630	30	2.05	2.0
<b>14</b>	174 460 <sup>c</sup>	153 000	105	2.82	2.0
	117 530 <sup>d</sup>	106 020	89	1.33	4.0
	105 850 <sup>a</sup>	94 950	27	2.86	2.0
<b>15</b>	172 310 <sup>c</sup>	130 360	95	3.74	2.0
	77 030 <sup>d</sup>	69 100	65	2.15	4.0
	103 330 <sup>a</sup>	97 800	18	1.21	2.0
<b>16</b>	161 070 <sup>c</sup>	154 520	61	1.40	2.0
	/ <sup>d</sup>	/	34	/	4.0
	75 660 <sup>a</sup>	71 070	24	2.51	2.0
<b>17</b>	157 750 <sup>c</sup>	136 700	73	3.19	2.0
	98 750 <sup>d</sup>	90 320	59	2.24	4.0
	95 000 <sup>a</sup>	88 740	43	2.51	2.0
<b>19</b>	136 300 <sup>c</sup>	127 050	119	1.87	2.0
	117 220 <sup>d</sup>	95 300	68	2.45	4.0

Eluents: as reported in note of Table 3.

#### 3.4. Note on thermodynamic performance of UHPC-Titan120-T<sub>ZWIT</sub>-1.9

As it was mentioned before, the new strategy to covalently bond teicoplanin to silica introduces a permanently charged ammonium fragment on the teicoplanin amino acid residue 1 (see Fig. 1A). The simultaneous presence of a carboxylate and an ammonium groups imparts a zwitterionic character to the CSP. This constitutes a unique characteristic of the UHPC-Titan120-T<sub>ZWIT</sub>-1.9 with respect to the commercially available teicoplanin-based CSPs, Chirobiotic T and Chirobiotic T2. In order to compare the thermodynamic properties of the UHPC-Titan120-T<sub>ZWIT</sub>-1.9 with those of Chirobiotic T and Chirobiotic T2, several chromatograms were recorded under identical experimental conditions on the different columns. The results of this study are given in Fig. 7(A, B) where the chromatograms obtained on two new UHPC-Titan120-T<sub>ZWIT</sub>-1.9 columns (20 mm  $\times$  4.6 mm and 50 mm  $\times$  4.6 mm, respectively), two

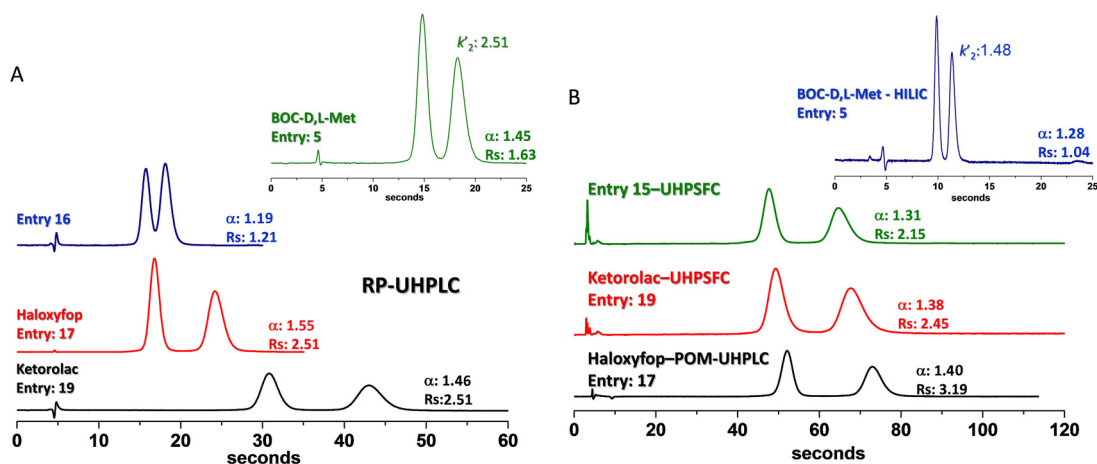


**Fig. 6.** Ultra-fast separations on a 1-cm long column. (A) Ketorolac **19**, haloxyfop **17**,  $\alpha$ -aryloxy acid **16** and N-BOC-*p*-L-Met **5** in RP (black, red, blue and green traces respectively) by using MeOH/H<sub>2</sub>O 85:15 + 20 mM ammonium acetate. (B) N-BOC-*p*-L-Met **5** in HILIC (blue line, ACN/H<sub>2</sub>O, 85/15), haloxyfop **17** in POM (ACN/MeOH 60:40 + 0.055% CH<sub>3</sub>COOH/0.03% TEA) at 2.0 mL/min (black chromatogram); ketorolac **19** and  $\alpha$ -aryloxy acid **15** in UHPSFC (CO<sub>2</sub>/A 60:40; A: MeOH/H<sub>2</sub>O 98:2 + 20 mM CH<sub>3</sub>COONH<sub>4</sub>) at flow-rate: 4.0 mL/min (red and green chromatograms). (For interpretation of the references to color in this figure legend, the reader is referred to the web version of this article.)

commercial Chirobiotic T (50 mm  $\times$  4.6 mm and 250 mm  $\times$  4.6 mm) and one commercial Chirobiotic T2 (250 mm  $\times$  4.6 mm) are compared. N-Fmoc-*p*-L-Ala and a peptoid of Phe (VL-0797) were used as probe compounds. These chromatograms show that both

enantiomers are significantly retained on the UHPC-Titan120-*T*<sub>ZWIT</sub>-1.9 columns, while they are only slightly retained or in some cases even excluded (due to Donnan interactions [42]) from the pores of the CSP particles on the Chirobiotic T and the Chirobiotic T2

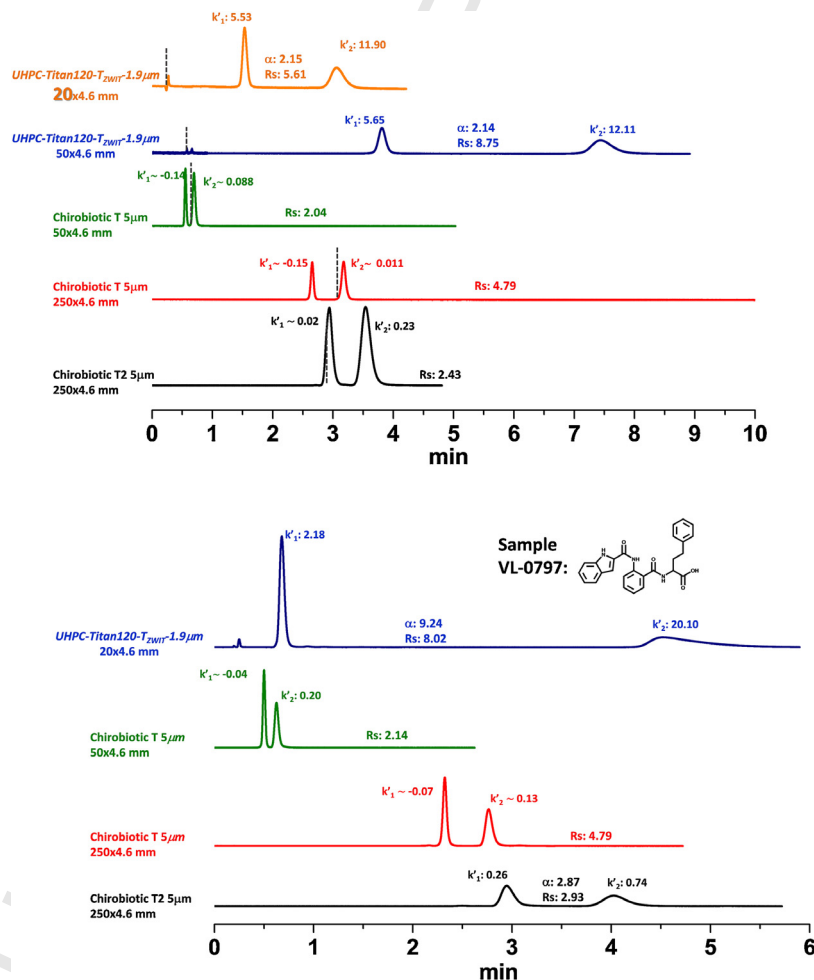


**Fig. 7.** Two representative comparisons between the 2-cm and 5-cm UHPC-Titan120-*T*<sub>ZWIT</sub>-1.9 (blue and orange lines), Chirobiotic T (50 mm  $\times$  4.6 mm, 5  $\mu$ m and 250 mm  $\times$  4.6 mm, 5  $\mu$ m, green and red lines respectively) and Chirobiotic T2 (250 mm  $\times$  4.6 mm, 5  $\mu$ m, black line). N-Fmoc-*p*-L-Ala and VL-0797 separations in RP condition (MeOH/H<sub>2</sub>O 85:15 + 20 mM CH<sub>3</sub>COONH<sub>4</sub>) and ACN/H<sub>2</sub>O 70:30 + 15 mM KH<sub>2</sub>PO<sub>4</sub> respectively; flow-rate 1.0 mL/min; *T*: 35  $^{\circ}$ C. Dashed line represents the void volume of each column. (For interpretation of the references to color in this figure legend, the reader is referred to the web version of this article.)

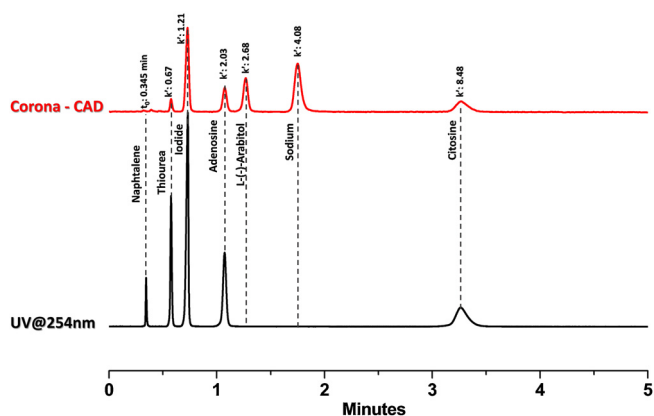


**Fig. 8.** Separation of naphthalene, thiourea, iodide ion, adenosine, L-arabitol, sodium ion, cytosine on 5-cm UHPC-Titan120-TZWIT-1.9. Elution condition: ACN/H<sub>2</sub>O 85:15 + 15 mM ammonium acetate; flow-rate: 1.5 mL/min; UV at 254 nm and Corona-CAD detectors. Corona chromatographic trace corrected for a delay time of 0.038 min.

column. The importance of Donnan effect to understand the exclusion of some enantiomers from teicoplanin-based CSPs obtained via ureido-linkage (such as the Chirobiotic T and T2 CSPs) was investigated in detail in [42]. In that work it was demonstrated that, under conditions very close to those of Fig. 7, these CSPs bear a negative charge due to the deprotonated carboxylic group. A negatively charged analyte is, under these conditions, excluded by the stationary phase due to Donnan repulsion effects [42]. On the contrary, on the UHPC-Titan120-TZWIT-1.9 these effects are absent.

As an additional test to evaluate the zwitterionic nature of the UHPC-Titan120-TZWIT-1.9 stationary phase, Fig. 8 reports the chromatogram of a mixture of hydrophobic, neutral polar and permanently charged compounds (NaI) under HILIC condition. Two different detectors (PDA and Corona-CAD) were used in series in order to detect also non-UV-absorbing compounds (e.g., Na<sup>+</sup>, L-arabitol, etc.). Interestingly, all analytes were baseline resolved, including sodium (Na<sup>+</sup>) and iodide (I<sup>-</sup>), which did not experience Donnan repulsion on the zwitterionic CSP. Thus, the retention of ionic species (positively or negatively charged) can be suitably modulated by changing the pH or the ionic strength of the mobile phase (data not shown). As a preliminary conclusion, we may state that a zwitterionic form of teicoplanin-based CSP has been obtained thanks to the introduction on the CSP of a new positively charged site (anion-exchange) in addition to the carboxylate group (weak cation-exchange) and the chiral carboxylate hydrogen-binding pocket. The zwitterionic character gives to this teicoplanin-based CSP unique multimodal/multipurpose properties opening unexpected opportunities in the field of separation of mixtures of charged, neutral chiral and achiral molecules.

#### 4. Conclusions

The new UHPC-Titan120-TZWIT-1.9 was prepared starting from the 1.9 μm fully porous Titan silica particles for applications in ultra-fast separations. The results demonstrate that fast and ultra-fast high performance chiral chromatography can take advantage of the use of sub-2 μm totally porous silica particles of narrow size distribution. Downsizing in column length, from 10-cm to 5-cm, 2-cm and 1-cm was easily possible maintaining high efficiency values and obtaining baseline separations. The enantiomers of N-BOC-D,L-methionine were successfully baseline separated in only 11 s in HILIC-UHPLC. The new UHPC-Titan120-TZWIT-1.9 represents a new multimodal/multipurpose chiral stationary phase and demonstrated wide possibilities of elution conditions: reversed phase, normal phase, polar organic mode and remarkably hydrophilic

interaction liquid chromatography and sub/supercritical fluid chromatography.

#### Conflict of interest

The authors declare no conflict of interest.

#### Acknowledgments

This work was supported by Sapienza University contract no. Q419 20122ATMNJ. The authors thank Waters s.p.a. (Milano, Italy) for providing UPC<sup>2</sup> instrumentation. The authors thank Dr. E. Bianchini, Department of Chemistry and Pharmaceutical Sciences, University of Ferrara, for elemental analysis measurements and Dr. A. Varnavas, Department of Chemical and Pharmaceutical Sciences, University of Trieste, to supply the peptoid VL-0797 sample.

#### Appendix A. Supplementary data

Supplementary data associated with this article can be found, in the online version, at <http://dx.doi.org/10.1016/j.chroma.2015.11.071>.

#### References

- [1] M. Lämmerhofer, W. Lindner, Quinine and quinidine derivatives as chiral selectors I. Brush type chiral stationary phases for high-performance liquid chromatography based on cinchona carbamates and their application as chiral anion exchangers, *J. Chromatogr. A* 741 (1996) 33–48.
- [2] N.M. Maier, L. Nicoletti, M. Lämmerhofer, W. Lindner, Enantioselective anion exchangers based on cinchona alkaloid-derived carbamates: influence of C8/C9 stereochemistry on chiral recognition, *Chirality* 11 (1999) 522–528.
- [3] C.V. Hoffmann, R. Pell, M. Lämmerhofer, W. Lindner, Synergistic effects on enantioselectivity of zwitterionic chiral stationary phases for separations of chiral acids, bases, and amino acids by HPLC, *Anal. Chem.* 80 (2008) 8780–8789.
- [4] C. Rosini, P. Altamura, D. Pini, C. Bertucci, G. Zullino, P. Salvadori, Cinchona alkaloids for preparing new, easily accessible chiral stationary phases: II. Resolution of binaphthol derivatives on silica-supported quinine, *J. Chromatogr.* 348 (1985) 79–87.
- [5] D.W. Armstrong, Y. Tang, S. Chen, Y. Zhou, C. Bagwill, J.-R. Chen, Macrocyclic antibiotics as a new class of chiral selectors for liquid chromatography, *Anal. Chem.* 66 (1994) 1473–1484.
- [6] A. Berthod, X.H. Chen, J.P. Kullman, D.W. Armstrong, F. Gasparrini, I. D'Acquarica, C. Villani, A. Carotti, Role of the carbohydrate moieties in chiral recognition on teicoplanin-based LC stationary phases, *Anal. Chem.* 72 (2000) 1767–1780.
- [7] I. D'Acquarica, F. Gasparrini, D. Misiti, M. Pierini, C. Villani, HPLC chiral stationary phases containing macrocyclic antibiotics: practical aspects and recognition mechanism, *Adv. Chromatogr.* 46 (2008) 109–173.
- [8] D.W. Armstrong, Y. Liu, K.H. Ekborgott, A covalently bonded teicoplanin chiral stationary phase for HPLC enantioseparations, *Chirality* 7 (1995) 474–497.
- [9] W.H. Pirkle, J.M. Finn, Chiral high-pressure liquid chromatographic stationary phases. 3. General resolution of aryl alkyl carbinols, *J. Org. Chem.* 46 (1981) 2935–2938.
- [10] W.H. Pirkle, C.J. Welch, B. Lamm, Design, synthesis, and evaluation of an improved enantioselective naproxen selector, *J. Org. Chem.* 57 (1992) 3854–3860.
- [11] F. Gasparrini, D. Misiti, M. Pierini, C. Villani, Enantioselective chromatography on brush-type chiral stationary phases containing totally synthetic selectors: theoretical aspects and practical applications, *J. Chromatogr. A* 724 (1996) 79–90.
- [12] A.M. Stalcup, S.-C. Chang, D.W. Armstrong, J. Pitha, (S)-2-Hydroxypropyl-β-cyclodextrin, a new chiral stationary phase for reversed-phase liquid chromatography, *J. Chromatogr.* 513 (1990) 181–194.
- [13] S.G. Allenmark, S. Andersson, P. Möller, D. Sanchez, A new class of network-polymeric chiral stationary phases, *Chirality* 7 (1995) 248–256.
- [14] Y. Okamoto, M. Kawashima, K. Hatada, Chromatographic resolution: XI. Controlled chiral recognition of cellulose triphenylcarbamate derivatives supported on silica gel, *J. Chromatogr.* 363 (1986) 173–186.
- [15] Y. Okamoto, S. Honda, I. Okamoto, H. Yuki, S. Murata, R. Noyori, H. Takaya, Novel packing material for optical resolution: (+)-poly(triphenylmethyl methacrylate) coated on macroporous silica gel, *J. Am. Chem. Soc.* 103 (1981) 6971–6973.
- [16] S. Allenmark, B. Bomgren, H. Borén, Direct liquid chromatographic separation of enantiomers on immobilized protein stationary phases: III. Optical resolution of a series of N-aryl-L-p-amino acids by high-performance liquid chromatography on bovine serum albumin covalently bound to silica, *J. Chromatogr.* 264 (1983) 63–68.

- [17] F. Gasparrini, D. Misiti, R. Rompietti, C. Villani, New hybrid polymeric liquid chromatography chiral stationary phase prepared by surface-initiated polymerization, *J. Chromatogr. A* 1064 (2005) 25–38.
- [18] D. Kotoni, C. Villani, D.S. Bell, D. Capitani, P. Campiglia, F. Gasparrini, Bidentate urea-based chiral selectors for enantioselective high performance liquid chromatography: synthesis and evaluation of “Crab-like” stationary phases, *J. Chromatogr. A* 1297 (2013) 157–167.
- [19] D. Mangelings, Y. Vander Heyden, Screening approaches for chiral separations, *Adv. Chromatogr.* 46 (2008) 175–210.
- [20] M.E. Andersson, D. Aslan, A. Clarke, J. Roeraade, G. Hagman, Evaluation of generic chiral liquid chromatography screens for pharmaceutical analysis, *J. Chromatogr. A* 1005 (2003) 83–101.
- [21] M.L. de la Puente, C.T. White, A. Rivera-Sagredo, J. Reilly, K. Burton, G. Harvey, Impact of normal-phase gradient elution in chiral chromatography: a novel, robust, efficient and rapid chiral screening procedure, *J. Chromatogr. A* 983 (2003) 101–114.
- [22] Y. Zhang, W. Watts, L. Nogle, O. McConnell, Rapid method development for chiral separation in drug discovery using multi-column parallel screening and circular dichroism signal pooling, *J. Chromatogr. A* 1049 (2004) 75–84.
- [23] M.M. Wong, W.B. Holzheuer, G.K. Webster, A comparison of HPLC and SFC chiral method development screening approaches for compounds of pharmaceutical interest, *Curr. Pharm. Anal.* 4 (2008) 101–105.
- [24] Z. Pirzada, M. Personick, M. Biba, X. Gong, L. Zhou, W. Schafer, C. Roussel, C.J. Welch, Systematic evaluation of new chiral stationary phases for supercritical fluid chromatography using a standard racemate library, *J. Chromatogr. A* 1217 (2010) 1134–1138.
- [25] P. Franco, T. Zhang, Finding the best separation for enantiomeric mixtures, *LCCG North Am.* 28 (2010) 818–822.
- [26] E.L. Regalado, C.J. Welch, Pushing the speed limit in enantioselective supercritical fluid chromatography, *J. Sep. Sci.* 38 (2015) 2826–2832.
- [27] C.J. Welch, E.L. Regalado, Estimating optimal time for fast chromatographic separations, *J. Sep. Sci.* 37 (2014) 2552–2558.
- [28] F. Ai, L. Li, S.-C. Ng, T.T.Y. Tan, Sub-1-micron mesoporous silica particles functionalized with cyclodextrin derivative for rapid enantioseparations on ultra-high pressure liquid chromatography, *J. Chromatogr. A* 1217 (2010) 7502–7506.
- [29] G. Cancelliere, A. Ciogli, I. D’Acquarica, F. Gasparrini, J. Kocergin, D. Misiti, M. Pierini, H. Ritchie, P. Simone, C. Villani, Transition from enantioselective high performance to ultra-high performance liquid chromatography: a case study of a brush-type chiral stationary phase based on sub-5-micron to sub-2-micron silica particles, *J. Chromatogr. A* 1217 (2010) 990–999.
- [30] D. Kotoni, A. Ciogli, C. Molinaro, I. D’Acquarica, J. Kocergin, T. Szczerba, H. Ritchie, C. Villani, F. Gasparrini, Introducing enantioselective ultrahigh-pressure liquid chromatography (eUHPLC): theoretical inspections and ultrafast separations on a new sub-2- $\mu\text{m}$  Whelk-O1 stationary phase, *Anal. Chem.* 84 (2012) 6805–6813.
- [31] A. Cavazzini, N. Marchetti, R. Guzzinati, M. Pierini, A. Ciogli, D. Kotoni, I. D’Acquarica, C. Villani, F. Gasparrini, Enantioselective separation by ultra-high-performance liquid chromatography, *TrAC* 63 (2014) 95–103.
- [32] L. Sciascera, O. Ismail, A. Ciogli, D. Kotoni, A. Cavazzini, L. Botta, T. Szczerba, J. Kocergin, C. Villani, F. Gasparrini, Expanding the potential of chiral chromatography for high-throughput screening of large compound libraries by means of sub-2  $\mu\text{m}$  Whelk-O 1 stationary phase in supercritical fluid conditions, *J. Chromatogr. A* 1383 (2015) 160–168.
- [33] Y. Min, Z. Sui, Z. Liang, L. Zhang, Y. Zhang, Teicoplanin bonded sub-2  $\mu\text{m}$  superficially porous particles for enantioselective separation of native amino acids, *J. Pharm. Biomed. Anal.* 114 (2015) 247–253.
- [34] D.C. Patel, Z.S. Breitbach, M.F. Wahab, C.L. Barhate, D.W. Armstrong, Gone in seconds: praxis, performance, and peculiarities of ultrafast chiral liquid chromatography with superficially porous particles, *Anal. Chem.* (2015), <http://dx.doi.org/10.1021/acs.analchem.1025b00715>.
- [35] F. Gritti, D.S. Bell, G. Guiochon, Particle size distribution and column efficiency. An ongoing debate revived with 1.9  $\mu\text{m}$  Titan-C18 particles, *J. Chromatogr. A* 1355 (2014) 179–192.
- [36] R.A. Henry, P. Ross, W.R. Betz, D.S. Bell, G. Parmar, W.K. Way, The importance of monodisperse silica in the evolution of UHPLC and HPLC column performance, *Am. Lab.* (2015), posted on the web: March 2015.
- [37] I. Halasz, M. Naefe, Influence of column parameters on peak broadening in high-pressure liquid chromatography, *Anal. Chem.* 44 (1972) 76–84.
- [38] D. Cabooter, A. Fanigliulo, G. Bellazzi, B. Allieri, A. Rottigni, G. Desmet, Relationship between the particle size distribution of commercial fully porous and superficially porous high performance liquid chromatography column packings and their chromatographic performance, *J. Chromatogr. A* 1217 (2010) 7074–7081.
- [39] F. Gritti, G. Guiochon, The quantitative impact of the mesopore size on the mass transfer mechanism of the new 1.9  $\mu\text{m}$  fully porous Titan-C18 particles. I: analysis of small molecules, *J. Chromatogr. A* 1384 (2015) 76–87.
- [40] F. Gritti, G. Guiochon, The rationale for the optimum efficiency of columns packed with new 1.9  $\mu\text{m}$  fully porous Titan-C18 particles: a detailed investigation of the intra-particle diffusivity, *J. Chromatogr. A* 1315 (2014) 164–178.
- [41] I. Ilisz, R. Berkecz, A. Péter, Retention mechanism of high-performance liquid chromatographic enantioselective separation on macrocyclicglycopeptide-based chiral stationary phases, *J. Chromatogr. A* 1216 (2009) 1845–1860.
- [42] A. Cavazzini, G. Nadalini, F. Dondi, F. Gasparrini, A. Ciogli, C. Villani, Study of mechanisms of chiral discrimination of amino acids and their derivatives on a teicoplanin-based chiral stationary phase, *J. Chromatogr. A* 1031 (2004) 143–158.
- [43] M. Bois-Choussy, L. Neuville, R. Beugelmans, J. Zhu, Synthesis of modified carbonyl binding pockets of vancomycin and teicoplanin, *J. Org. Chem.* 61 (1996) 9309–9322.
- [44] N.J. Economou, I.J. Zentner, E. Lazo, J. Jakoncic, V. Stojanoff, S.D. Weeks, K.C. Grasty, S. Cocklin, P.J. Loll, Structure of the complex between teicoplanin and a bacterial cell-wall peptide: use of a carrier-protein approach, *Acta Crystallogr. D* 69 (2013) 520–533.
- [45] S. Han, B.V. Le, H.S. Hajare, R.H.G. Baxter, S.J. Miller, X-ray crystal structure of teicoplanin A-2 bound to a catalytic peptide sequence via the carrier protein strategy, *J. Org. Chem.* 79 (2014) 8550–8556.
- [46] A. Ciogli, D. Kotoni, F. Gasparrini, M. Pierini, C. Villani, Chiral supramolecular selectors for enantiomer differentiation in liquid chromatography, *Top. Curr. Chem.* 340 (2013) 73–106.
- [47] C.L. Barhate, M.F. Wahab, Z.S. Breitbach, D.S. Bell, D.W. Armstrong, High efficiency, narrow particle size distribution, sub-2  $\mu\text{m}$  based macrocyclic glycopeptide chiral stationary phases in HPLC and SFC, *Anal. Chim. Acta* (2015), <http://dx.doi.org/10.1016/j.jaca.2015.09.048>.
- [48] F. Gritti, G. Guiochon, Accurate measurements of peak variances: importance of this accuracy in the determination of the true corrected plate heights of chromatographic columns, *J. Chromatogr. A* 1218 (2011) 4452–4461.
- [49] A. Grand-Guillaume Perrenoud, J.-L. Veuthey, D. Guillaume, Comparison of ultra-high performance supercritical fluid chromatography and ultra-high performance liquid chromatography for the analysis of pharmaceutical compounds, *J. Chromatogr. A* 1266 (2012) 158–167.
- [50] A. Grand-Guillaume Perrenoud, C. Hamman, M. Goel, J.-L. Veuthey, D. Guillaume, S. Fekete, Maximizing kinetic performance in supercritical fluid chromatography using state-of-the-art instruments, *J. Chromatogr. A* 1314 (2013) 288–297.
- [51] R.A. Shalliker, B.S. Broyles, G. Guiochon, Physical evidence of two wall effects in liquid chromatography, *J. Chromatogr. A* 888 (2000) 1–12.